2013 IEEE Point-of-Care Healthcare Technologies (PHT)
Bangalore, India, 16 - 18 January, 2013

A Novel Algorithm for CT-Ultrasound Registration

Lijian Xu, Jun Liu, Weiwei Zhan, and Lixu Gu

Abstract—**The fusion of ultrasound (US) with CT plays a vital role in clinical diagnosis and image guided intervention. A registration framework between preoperative CT and tracked 2D intraoperative US is proposed here for hepatic intervention. After a landmark based registration method is carried out to get the initial registration, a simulation model of US from CT scan is developed to simulate the major US effects. The innovation is incorporating spatial and intensity scale information in a new similarity metric, which is to register the selected US image containing crucial anatomical features and the simulated US from CT. Experiments of 5 patients illustrate that our registration method achieved an average FRE and TRE of 3.81 ± 1.16 mm and 4.13 ± 1.27 mm.**

I. Introduction

Radio frequency (RF) ablation is now considered as a reliable minimal invasive procedure to treat small liver tumor, which provides similar long-term treatment outcome as surgical resection [1-2]. During the operation of RF ablation, one or multiple needles are inserted into the tumor through the skin. An electrical current is conducted through the needle, creating heat at the needle tip to cause coagulative necrosis of the tumor tissue. Preoperative planning and precise localization of the needle is extremely important in the procedure in order to avoid the destruction of neighboring normal tissues. Both US and CT can be used as the intraoperative guidance modality. However, CT scan cannot provide real time guidance and it exposes patients and clinicians to a substantial amount of radiation. The procedure of RF ablation is usually performed under US guidance. However, there are occasions when the lesions can't be visualized clearly in US, but can be seen in CT or MRI. In these cases, it would be desirable to register the preoperative CT/MRI and intraoperative US to improve the accuracy of the guidance.

Much research on CT/MRI to US registration for liver surgery has been performed with feature [3-5], or intensity based techniques [6-9]. However, the current achievements are still difficult to satisfy the clinical demand of automated and accurate registration between the two modalities. The theoretical difficulty in aligning CT and US images is that the two modalities generate images of very different appearance due to the incoherent intensity information, making it challenging to develop a similarity metric between CT and US. In this study, we present a CT-US registration framework, in which the landmark based registration method is utilized to get initial transformation that contributes to narrowing the optimization, while the image based registration method helps to improve the accuracy. The novelty is the presentation of a new similarity metric which incorporates intensity and spatial information of the images. The new metric has been proven effective in common registration cases including CT-US alignment. Specific image preprocessing and simulation methods are also used to increase the similarity between the two modalities, which improve the accuracy of registration. Experiments indicate that our registration framework is effective for CT-US alignment in US-guided liver intervention.

Manuscript received September 25, 2012. This work was partially supported by the Chinese Nature Science Foundation (project #61271318). Asterisk indicates corresponding author.

Lijian Xu and *Lixu Gu are with the Med-X Research Institute, Shanghai Jiaotong University, Shanghai 200030, China (e-mail: gulixu@ sjtu.edu.cn).

Jun Liu and Weiwei Zhan are with the Department of Ultrasound, Ruijing Hospital, Shanghai Jiaotong University, Shanghai, China (e-mail: liujunqwer@hotmail.com).

II. Material and Methods

A. US Simulation from CT

The simulation of US from CT is based on the US physics. The phenomena like reflection, refraction and diffraction will occur when US wave goes through the media of different densities. A simple beam-based model is developed, considering only the reflection and attenuate properties [10].

● Reflection

US is partially reflected at the interface of two tissues of different acoustic impedances when traveling through a piecewise homogenous medium. The acoustic impedance $Z = \rho c$, is defined as the product of density of the media ρ and the speed of sound c in the medium. Not considering the bone and air tissues, a constant speed of sound is assumed since the speed of sound is about 1540m/s in soft tissue. The equations based on the US physics are given as

$$\alpha_R = \frac{I_r}{I_i} = (\cos\theta)^n \left(\frac{Z_2 - Z_1}{Z_2 + Z_1}\right)^2 \quad (1)$$

$$\Delta r(x,d) = (\cos\theta)^n \left(\frac{\nabla Z(x)}{2 \cdot Z(x)}\right)^2 = \left(d^T \frac{\nabla \mu(x)}{|\nabla \mu(x)|}\right)^n \left(\frac{\nabla \mu(x)}{2\mu(x)}\right)^2 \quad (2)$$

where 1) α_R is the ratio of reflected intensity to incident intensity, I_r and I_i are the intensities of reflected and incident wave beam respectively; 2) $\Delta r(x,d)$ is the incremental reflected intensity, $\mu(x)$ is the attenuate value at location x, $\nabla \mu(x)$ is the space incremental, d is the unit vector in the direction of ultrasound wave propagation, and

$\cos\theta$ equals to the dot product of d and the normalized gradient vector. As tissue density ρ is proportional to the attenuation coefficient μ and acoustic impedance Z respectively, we assume that μ is proportional to Z.

● Attenuation

The procedure of attenuation can be described by Beer-Lambert-Law. The discrete expressions of the law and the intensity received by transducer are defined as following:

$$\frac{I_i}{I_0} = [\prod_{i=1}^{n} \exp(-\lambda \frac{|\nabla \mu(x_i)|}{2\mu(x_i)})]^2 \quad (3)$$

$$I_r(x) = I_0[\prod_{i=1}^{n} \exp(-\lambda \frac{|\nabla \mu(x_i)|}{2\mu(x_i)})]^2 (\mathrm{d}^T \nabla \mu(x)) \frac{|\nabla \mu(x)|}{(2\mu(x))^2} \quad (4)$$

where I_0 is the initial intensity, and λ is the distance between sampling pixels.

As shown in Fig. 1(b), the tissue boundaries are enhanced due to the large-scale US reflection and the tissues below bone are completely eliminated due to the high reflection ratio at the interface. Fig. 1(d) demonstrates the simulated US image from CT, which prepares for the image based registration method.

B. Similarity Measure

Mutual Information (MI) derives from communication theory, measuring the statistical dependence between two random variables or the amount of information that one variable contains about the other [11]. The MI of the random variables A and B can be expressed as follows:

$$MI(A,B) = H(A) + H(B) - H(A,B) \quad (5)$$

with $H(A)$ and $H(B)$ denoting the marginal entropy of A and B respectively, $H(A,B)$ their joint entropy, and $H(A|B)$ the conditional entropy of A given B.

The MI based registration method has proven to be a flexible and robust intensity based method especially for multi-modality registration [11–14]. However, present methods including MI based ones can't guarantee good results for CT-US registration due to the low quality of US image. One possible reason for this is the ignorance of the spatial information contained in the images such as the edges and corners that might be useful in the image registration. Incorporating the dependence of the grey values of neighboring voxels, what we term the spatial information of the images, could improve registration [12]. A similarity metric incorporating spatial and intensity scale information is presented in this paper. MI not only evaluates the similarity between intensity distribution but also the spatial information distributions of two images.

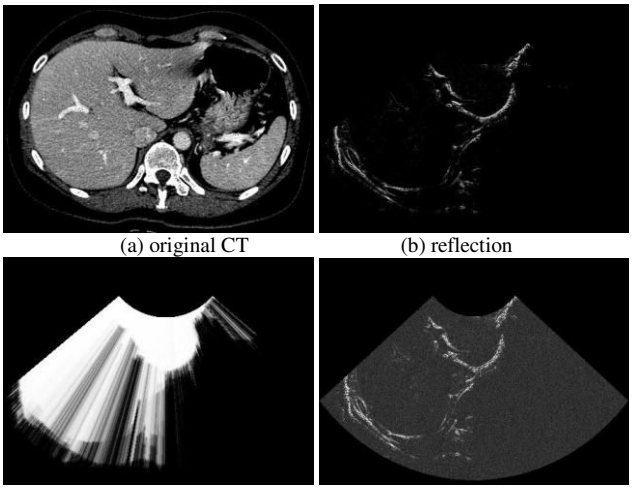

(a) original CT (b) reflection

(c) transmission (d) simulation result

Fig. 1 Simulation of US effects from CT for a curvilinear virtual probe. The original image is showed in (a). The simulated reflection image, transmission image and final image are depicted in (b), (c) and (d).

Spatial information can be depicted by many ways such as gradient or normal vector (NV). The normal vector information (NVI) is used here to represent the spatial information. A contour line or isosurface can be drawn based on the intensity value from the image and the NV is the vector which is perpendicular to the isosurface of one pixel in the image. The NV value can be computed from the direction value of gradient of image. Three NV components along x, y and z axes can be extracted from a 3D image. Zhuang et al. [15] have demonstrated that the NVI images of the aligned images are quite similar whatever the same or different modalities.

There are mainly two ways to combine the intensity and spatial information into a single similarity measure. In [16], the algorithm uses combination of the marginal and joint entropies of the images as MI. The angle between the gradient vectors of each point of the images is the gradient information. As a resulting measure this algorithm multiplies the gradient and mutual measures. In the second type of methods [17], new pixel value is computed by addition of the normalized original pixel value and its gradient magnitude value. Then MI is utilized to measure the new combined images. In sum, MI does not utilize the inherent spatial information of images for the first method, and the second method is not suitable for multi-modality registration since the intensity value in multi-modality images is totally different but the gradient magnitude value has much similar value. Such simple summation of the intensity and spatial information may decrease the final MI value. To solve the mentioned problems, a new combination strategy of the intensity and spatial information is proposed, which is to summate the MI value of intensity information and MI value of spatial information. The final metric value can be achieved by Equation (6).

$$Metric(A,B) = MI(A,B) + \sum_{i}^{n} MI(NV_{Ai}, NV_{Bi}) \quad (6)$$

Even though the intensity value in multi-modality images is different, both the MI value of intensity information and MI of spatial information represent the similarity of the images. So the summation of respective MI value of the intensity and spatial information will increase the total similarity value for multi-modality registration. Our similarity metric has been evaluated in many cases of medical image registration and the preliminary results are satisfactory [18].

III. RESULTS

A study of 5 patients that have lesions in the liver is performed to evaluate the methods. A triphasic helical double-Source computed tomography scanner (Siemens, Ruijing hospital) is used. The US image is obtained from GE E9 US machine with a localized calibrated probe. All the CT and US data are acquired during breath-hold on inspiration. Our system employs an electromagnetic tracking devices (AURORA, Northern Digital Inc., Canada) and an US probe [19]. The US probe attached with a NDI EM sensor (6 degrees of freedom, 6DOF) is calibrated in order to introduce US image into our system. The real-time US images are fed into a PC with a frame grabber.

Fig. 2(a) depicts the fusion image of CT volume with US by our methods. Outlines with digital marks (1: subcutaneous soft tissue layer, red; 2: spine, brown) show corresponding position in the image pair. The clinician confirms that the corresponding features including subcutaneous soft tissue layer and spine can be seen roughly to be aligned in the images. In order to show more details, the US frame and the corresponding slice from the CT volume after it has been resampled by the final registration matrix are shown in Fig. 2(b). Fig. 2(b) show a color overlay of CT (blue) and US (white). They depict the fusion images of US image with the resampled 2D CT slice by the registration methods. As shown in Fig. 2(b), arrows (3: hepatic portal vessels, green; 4: hepatic outline, purple 5: abdominal aorta, orange) which are labeled by expert show corresponding position in the images.

The Bronze Standard has been developed to assess the registration results by carefully selecting fiducial and target corresponding points in CT and US images. 4 corresponding vessel bifurcations are used as the fiducial landmarks, while the centers of the lesions are defined as the target points. Table 1 demonstrates the accuracy, robustness, and computation speed results of 5 patients including 100 US frames. The average and standard deviation (SD) of root mean square of the residual distances of the fiducial and target points are listed. The fiducial and target registration errors are expressed as FRE and TRE respectively. The landmark based registration method achieves an average FRE and TRE of 5.08 mm and 10.44 mm. These are improved to an average FRE and TRE of 3.81 mm and 4.13 mm after running our image based registration method. An average of 76 s is taken to perform the whole workflow. Our methods succeed to improve the accuracy in 97% of the cases if the FRE of the landmark registration is less than 15 mm. The alignment does not improve in the left cases is due to insufficient information in the US image. The acquisition of US images on a desired region containing vessel and hepatic outline information would increase the success ratio of registration.

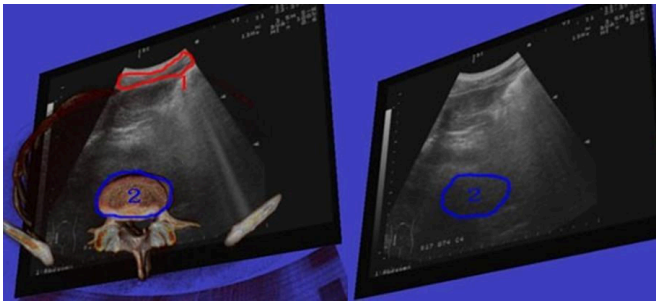

(a)

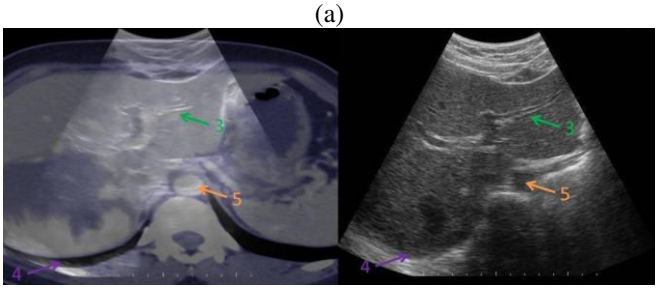

(b)

Fig. 2 The fusion images of CT volume (a) and resampled slice (b) with US. Digital marks (1: subcutaneous soft tissue layer, red; 2: spine, brown; 3: hepatic portal vessels, green; 4: hepatic outline, purple; 5: abdominal aorta, orange).

Table 1 Average and SD of FRE and TRE (mm), Failure rate, total time of the workflow (seconds)

	Initial		Final		SD		Failure rate	Total time
	FRE	TRE	FRE	TRE	FRE	TRE		
1	4.25	9.73	2.81	3.54	0.87	1.04	5%	68
2	3.84	8.14	3.54	3.85	1.18	1.27	0%	79
3	5.73	11.24	4.02	4.23	1.13	1.26	0%	71
4	5.41	12.86	4.13	4.41	1.54	1.63	10%	80
5	6.19	10.27	4.59	4.64	1.09	1.17	0%	82
	5.08	10.44	3.81	4.13	1.16	1.27	3%	76

In sum, our methods provide a simple workflow and more accurate multimodal fusion for the clinical diagnosis. It is easy for the expert to select several fiducials in both CT and US images with the convenient interaction provided by our system. Our methods achieve an average FRE and TRE of 3.81 ± 1.16 mm and 4.13 ± 1.27 mm.

IV. DISCUSSION AND CONCLUSION

To our knowledge, there are scarce fully automated CT-US registration workflows applied in clinical liver application. The accurate registration still depends on an initial landmark registration that requires some manual effort to define fiducials of the patient. In this study, a landmark based registration method is combined with the image based registration method. The landmark based registration method is always accredited for its efficient computation, but it fails to guarantee good registration results. On the other hand, the image based registration method helps to improve the accuracy and avoid extensive manual steps. However, it always relies on the optimization of a parameter space which is prone to getting stuck in local optima, resulting in a large mismatch. The combination of the above methods has a

trade-off between minimal interaction, speed, accuracy and robustness.

A registration framework between preoperative CT and tracked 2D intraoperative US images of liver has been proposed in this paper. Our method mainly consists of three aspects. Firstly, a landmark based registration method is performed to obtain initial transformation between the CT and US images. Secondly, the simulation of US from CT is employed to make the two modalities more similar in appearance. Thirdly, a new similarity metric incorporating spatial and intensity scale information is presented to register the simulated US and the real US. Our methods are evaluated by 5 patients data and the registration results are compared to the Bronze Standard defined by a clinical expert. Experiments demonstrate that our methods achieve an average TRE of 4.13 mm with an execution time of about 76 s, which provide higher accuracy and simplify the procedure for clinical applications. Involved clinicians confirmed that it is acceptable in medical diagnosis and clinical RF ablation.

REFERENCES

[1] D. Haemmerich, "Biophysics of radiofrequency ablation," Critical Reviews in Biomedical Engineering, vol. 38, no. 1, pp. 53–63, 2010.

[2] S. N. Goldberg, "Radiofrequency tumor ablation: principles and techniques," European Journal of Ultrasound, vol. 13, no. 2, pp. 129–147, Jun. 2001.

[3] B. Porter, D. Rubens, and J. Strang, "Three-dimensional registration and fusion of ultrasound and MRI using major vessels as fiducial markers," IEEE Transactions on Medical Imaging, vol. 20, no. 4, pp. 354–359, 2001.

[4] G. Penney, J. Blackall, and D. Hayashi, "Overview of an ultrasound to CT or MR registration system for use in thermal ablation of liver metastases," Proc. Medical Image Understanding and Analysis, pp. 7–10, 2001.

[5] S. Aylward and J. Jomier, "Intraoperative 3D ultrasound augmentation," Proc. IEEE International Symposium on Biomedical Imaging, pp. 421–424, 2002.

[6] G. P. Penney, J. M. Blackall, M. S. Hamady, T. Sabharwal, a. Adam, and D. J. Hawkes, "Registration of freehand 3D ultrasound and magnetic resonance liver images," Medical Image Analysis, vol. 8, no. 1, pp. 81–91, Mar. 2004.

[7] A. Leroy, P. Mozer, and Y. Payan, "Rigid registration of freehand 3D ultrasound and CT-scan kidney images," Medical Image Computing and Computer-Assisted Intervention—MICCAI 2004, vol. 3216, pp. 837–844, 2004.

[8] W. Wein, S. Brunke, A. Khamene, M. R. Callstrom, and N. Navab, "Automatic CT-ultrasound registration for diagnostic imaging and image-guided intervention," Medical image analysis, vol. 12, no. 5, pp. 577–85, Oct. 2008.

[9] T. Lange, N. Papenberg, S. Heldmann, J. Modersitzki, B. Fischer, H. Lamecker, and P. M. Schlag, "3D ultrasound-CT registration of the liver using combined landmark-intensity information," International journal of computer assisted radiology and surgery, vol. 4, no. 1, pp. 79–88, Jan. 2009.

[10] O. Kutter, R. Shams, and N. Navab, "Visualization and GPU-accelerated simulation of medical ultrasound from CT images," Computer methods and programs in biomedicine, vol. 94, no. 3, pp. 250–66, Jun. 2009.

[11] P. Viola, "Alignment by maximization of mutual information," International journal of computer vision, vol. 24, no. 2, pp. 137–154, 1997.

[12] J. P. W. Pluim, J. B. A. Maintz, and M. a Viergever, "Mutual-information-based registration of medical images: a survey.," IEEE Transactions on Medical Imaging, vol. 22, no. 8, pp. 986–1004, Aug. 2003.

[13] D. Loeckx, P. Slagmolen, F. Maes, D. Vandermeulen, and P. Suetens, "Nonrigid image registration using conditional mutual information," IEEE Transactions on Medical Imaging, vol. 29, no. 1, pp. 19–29, 2010.

[14] F. Maes, A. Collignon, and D. Vandermeulen, "Multimodality image registration by maximization of mutual information," IEEE Transaction on Medical Imaging, vol. 16, no. 2, pp. 187–198, 1997.

[15] X. Zhuang and L. Gu, "Normal Vector Information Registration and Comparisons with Mutual Information," International Conference of the IEEE Engineering in Medicine and Biology Society, pp. 3827–3830, Aug. 2006.

[16] J. P. Pluim, J. B. Maintz, and M. a Viergever, "Image registration by maximization of combined mutual information and gradient information.," IEEE Transactions on Medical Imaging, vol. 19, no. 8, pp. 809–14, Aug. 2000.

[17] K. A. L. Cheah, T.C. and Shanmugam, S.A. and Mann, "Medical Image Registration by Maximizing Mutual Information Based on Combination of Intensity and Gradient Information," Biomedical Engineering (ICoBE), 2012 International Conference, pp. 368 – 372, February. 2012.

[18] Y. P. He and L. X. Gu, Medical Image Registration Using Normal Vector and Intensity Value. International Conference on Intelligent Computation and Biomedical Instrumentation, pp. 46–49, 2011.

[19] J. Cai, Z. Luo, L. Gu, R. Xu, and Q. Zhao, "The implementation of an integrated computer-assisted system for minimally invasive cardiac surgery," The International Journal of Medical Robotics and Computer Assisted Surgery, vol. 6, no. 1, pp. 102–112, 2010.